

Tensile and fatigue strength of hydrogen-treated Ti-6Al-4V alloy

D. H. KOHN*, P. DUCHEYNE

Department of Bioengineering, University of Pennsylvania, Philadelphia, Pennsylvania 19104-6392, USA

Tensile, fatigue and fractographic data on Ti-6Al-4V microstructures attained through a series of post- β -annealing treatments which used hydrogen as a temporary alloying element are presented. Hydrogen-alloying treatments break up the continuous grain boundary α and colony structure, and produce a homogeneous microstructure consisting of refined α -grains in a matrix of discontinuous β . These changes in microstructural morphology result in significant increases of the yield strength (974 to 1119 MPa), ultimate strength (1025 to 1152 MPa) and high cycle fatigue strength (643 to 669 MPa) compared to respective values for lamellar microstructures (902, 994, 497 MPa). The strengths are also significantly greater than the strengths of equiaxed microstructures (914, 1000, 590 MPa). The strengths of hydrogen-alloy treated samples are therefore superior to strengths attainable via other thermal cycling techniques.

The fatigue fracture surfaces of the hydrogen-alloy treated samples were topographically similar to equiaxed samples. Fatigue crack initiation was characterized by faceted regions. As crack length and ΔK increased, the crack surface changed to a rounded, ductile topology, with microcracks and locally striated regions. Fracture primarily followed the α - β interfaces. This is rationalized by the fact that hydrogen-alloyed microstructures are very fine Widmanstätten microstructures having reduced aspect ratios, and these microstructures fail along α - β interfaces.

1. Introduction

The wide applicability of titanium and its alloys has necessitated tailoring their mechanical properties to appropriate structural needs. This has led to prolific research into the processing-structure-property relationships for titanium alloys [1-7].

Most mechanical properties of $\alpha + \beta$ titanium alloys, such as tensile strength and ductility, fracture toughness, fatigue strength and fatigue crack growth rate, are determined primarily by the amount, size, shape and distribution of the α and β phases and the density of α - β interfaces. A small α -grain size decreases the available reversible slip length, a critical parameter for fatigue crack initiation resistance. Minimizing the volume fraction of the β -phase decreases the length and density of α - β interfaces, areas prone to microstructural damage accumulation. Equiaxed microstructures, therefore, which typically have a small ($< 20 \mu\text{m}$) α -grain size, a well dispersed β -phase and a small α - β interface area, resist fatigue crack initiation well, and have excellent high cycle fatigue strength [3, 8-10]. In contrast, lamellar microstructures, have more continuous α - β interfaces and more oriented colonies than equiaxed microstructures. Slip is thus easily transmitted from one plate to another, and the effective slip length is the colony size rather

than the grain size [2, 9]. The increased slip length causes a strain intensification and therefore lower resistance to fatigue crack initiation and a lower fatigue strength.

Many processing conditions result in the formation of a lamellar microstructure, and as a consequence, a relatively low fatigue strength. Two important examples are found in the field of orthopaedic implants. The concept of implant fixation via bony ingrowth into the interstices of a porous surface layer sintered to a dense Ti-6Al-4V core has gained popularity [11, 12]. The porous coating and substrate are, however, typically bonded by a β -sintering treatment, which transforms the equiaxed microstructure into a lamellar microstructure. A second example is found in the increasing use of cast titanium alloys for prosthetic purposes [7]. Cast and hot isostatically pressed (HIPed) titanium components have a lower fatigue strength than forged components [7, 13, 14]. The relatively lower fatigue strength of cast titanium is due to the transformation of β to lamellar $\alpha + \beta$, upon cooling from the melt temperature through the $\beta \leftrightarrow \alpha + \beta$ transition temperature.

For net shapes with lamellar microstructures, a long-standing problem has been relieving the lamellar microstructure, without any adjuvant mechanical

*Present address: Department of Biological and Materials Sciences, School of Dentistry, The University of Michigan, Ann Arbor, MI 48109-1078, USA

TABLE I Chemical composition and mechanical properties of as-received Ti-6Al-4V bar material

Element (wt%)	N ₂	C	H ₂	Fe	O ₂	B	Cu	Si	Al	V
	0.018	0.014	0.009	0.16	0.12	0.001	0.002	0.13	6.1	4.2
Yield Strength (MPa)			893							
Ultimate Strength (MPa)			993							
Elongation (%)			18							
Reduction in Area (%)			42							

Chemical analysis and mechanical data supplied by Titanium Metals Corporation of America, Henderson, Nevada, USA

working, to improve high cycle fatigue strength. Until recently, there was no effective way to fully eliminate microstructural lamellarity in titanium alloys such that fatigue strengths would be equivalent to the fatigue strengths of equiaxed microstructures. With the advent of hydrogen as a temporary alloying element, however, a unique class of microstructures was created. These microstructures are finer than equiaxed microstructures and have superior tensile and fatigue strength [10, 15–20]. The key step in the treatment sequence is a eutectoid decomposition reaction, in which eutectoid α nucleates from the prior β -grains [15]. A eutectoid decomposition occurs because hydrogen, a β -stabilizer, lowers the $\alpha + \beta \leftrightarrow \beta$ transformation temperature to energetically favour a eutectoid phase transformation. These treatments have proven to be equally effective for cast [10, 16–18], powder [16–18, 21] and mill annealed Ti-6Al-4V [15, 17, 18].

The objectives of this research were to formulate a series of hydrogen-alloying treatments, that would relieve the lamellar microstructure developed from β -annealing and improve fatigue strength. A discussion of the microstructural morphology, physical metallurgy and phase transformations which produce this unique class of refined microstructures are presented in separate papers [19, 20]. The present paper focuses on the mechanical property evaluation of these hydrogen-alloy treated (HAT) microstructures, and for the first time, presents fractographic data on this unique class of microstructure.

2. Methods and materials

2.1. Materials and microstructural morphologies

The material used for the thermo chemical treatments and mechanical testing was 15.6 mm diameter forged, annealed, extra low interstitial (ELI) grade Ti-6Al-4V bar material. The chemical composition and mechanical properties (Table I), conformed to ASTM F136–84 [22].

Specimen groups were categorized by one of five microstructures: equiaxed (EA) (Fig. 1a), lamellar (L) (Fig. 1b) and three post- β -annealing hydrogen-alloying treatments: HAT-1, HAT-2 and HAT-3 (Fig. 2). Table II summarizes the thermal and thermochemical treatments used to derive each of the microstructures.

2.2. Tensile tests

Following the final thermal-thermochemical treatment, the bars were machined (Metcut Research Asso-

ciates, Cincinnati, OH) into tensile samples with a total length of 68.75 mm, a gauge length of 31.25 mm, and a gauge diameter of 6.25 mm. The specimen design, testing procedure and data reduction conformed to ASTM E8-85 [23]. Three to six samples per treatment condition were tested to failure on a closed-loop servo-hydraulic mechanical testing machine (Instron Model 1331) or an electro-mechanical testing machine (Instron Model 1361), under load control, at a constant strain rate of 0.5 mm min^{-1} . A strain gauge extensometer (Instron Model 2620-524) was used to record elongation. Load-elongation data were recorded on an x - y recorder (HP/Moseley Division-Moseley Autograf 7001AR), stress-strain curves were developed and yield strength, ultimate tensile strength,

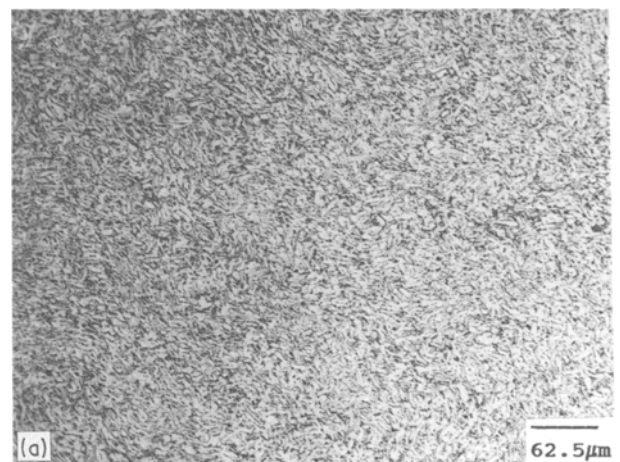


Figure 1 Light micrographs of (a) equiaxed and (b) lamellar Ti-6Al-4V. Equiaxed microstructures are characterized by small, rounded α -grains, with aspect ratios near unity and a dispersion of β at primary α grain boundaries. Lamellar microstructures are characterized by α -platelets in a β matrix, with grain boundary α .

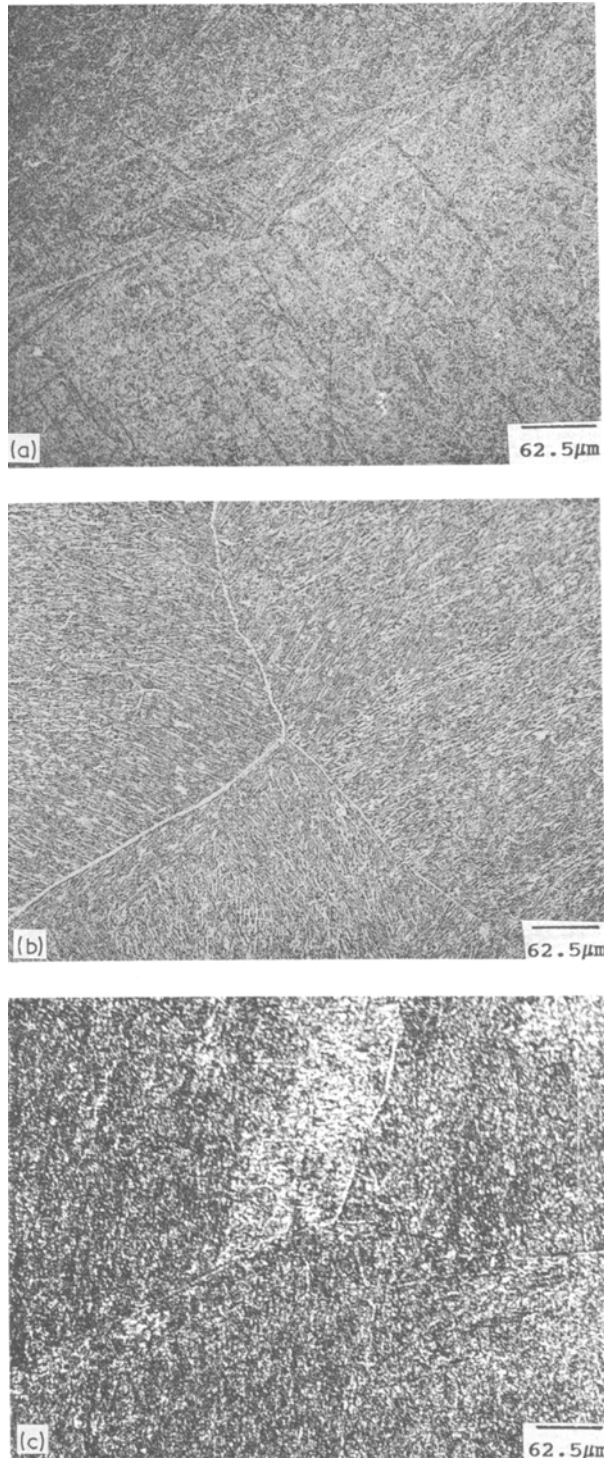


Figure 2 Light micrographs of Ti-6Al-4V subjected to post-sintering hydrogen-alloying treatments: (a) HAT-1: 850°C-0.5 h in H₂-650°C-16 h in vacuum, (b) HAT-2: 850°C-0.5 h in H₂-590°C-4 h in Ar-800°C-2 h in vacuum, (c) HAT-3: 850°C-0.5 h in H₂-590°C-4 h in Ar-775°C-4 h in vacuum. HAT microstructures are characterized by a fine, uniform $\alpha + \beta$ microstructure, resembling a Widmanstätten microstructure with a reduced aspect ratio.

total percent elongation and percent reduction in area at fracture were calculated.

2.3. Fatigue tests

Fatigue tests were performed on specimens in one of four microstructural conditions: EA, L, HAT-1 or HAT-3. After the final heat treatment, the rods were

machined into hour-glass specimens having a minimum gauge section diameter of 6.25 mm, and polished (Metcut Research Associates, Cincinnati, OH). The specimens and testing procedure conformed to ASTM E466-82 [24].

Rotating beam (fully reversed bending, $R = -1$) high-cycle fatigue tests were performed on an RBF-200 testing machine (Fatigue Dynamics, Inc., Dearborn, MI). Testing was conducted in air, at room temperature, at 100 to 130 Hz. Fifteen samples per treatment condition, unless noted otherwise, were tested to determine fatigue strength, by the staircase method [25, 26]. The initial applied stress (S_0) was an estimate of the fatigue strength. If the first specimen survived for 10^7 cycles, the second specimen was tested at a higher stress ($S_0 + d$), where d is a stress increment of 17.25 MPa (2.5 ksi). If the first specimen failed, the second specimen was tested at a lower stress ($S_0 - d$). Specimens were tested sequentially, each tested at one stress increment above or one decrement below the stress that the previous specimen was tested at. Stress levels and corresponding cycles to failure were recorded and statistical analysis of the fatigue strengths was performed, as described by Collins [26].

Fracture morphologies were investigated using optical microscopy (Nikon type 114), stereomicroscopy (Nikon type 104) and scanning electron microscopy (SEM) (Philips 500). Following SEM analysis, samples were sectioned with a low speed diamond saw (South Bay Technology Model 650) perpendicular to the fracture surface, a short distance from the crack initiation site. The cut face of the samples were then ground and polished, to investigate the microstructure directly under the fracture.

3. Results

3.1. Tensile properties

Average tensile data for each microstructural group tested are presented in Table III and the results of Student's t-tests to determine the statistical significance between tensile properties are listed in Table IV.

Fatigue data for each of the microstructural groups tested are presented in Table V. Student's t-tests were used to determine the statistical significance between the mean fatigue strengths of the different microstructures (Table VI). Since the staircase method prescribes that the mean fatigue strength be calculated from the lesser of the two populations of results (i.e. either failures or runouts), these levels of significance are conservative estimates.

4. Discussion

The tensile and fatigue strengths of the hydrogen-alloy treated microstructures were significantly greater than the tensile and fatigue strengths of both the lamellar and equiaxed microstructures. These strength values are amongst the highest reported for Ti-6Al-4V [3, 4, 9, 10, 14, 15].

Parameters affecting fatigue strengths, other than microstructure (texture, interstitials and surface roughness) were controlled for, such that the only

TABLE II Summary of thermo chemical treatments

Structure	Thermal-Thermochemical cycle	Average α -grain size (μm)
Equiaxed	As-received (Forged-Annealed)	3.40 (0.51)
Lamellar	β -annealing: 1370 °C-4 h-in vac-FC	4.00 (1.57)
HAT-1	Hydrogenation: 850 °C-0.5 h in H_2 -FC/ Dehydrogenation: 650 °C-16 h in vac-FC	0.91 (0.07)
HAT-2	Hydrogenation: 850 °C-0.5 h in H_2 / Eutectoid decomposition: 590 °C-4 h in Ar-FC/ Dehydrogenation: 800 °C-2 h in vac-FC	1.17 (0.06)
HAT-3	Hydrogenation: 850 °C-0.5 h in H_2 / Eutectoid decomposition: 590 °C-4 h in Ar-FC/ Dehydrogenation: 775 °C-4 h in vac - FC	1.26 (0.29)

FC = furnace cool, standard deviations in ()

material variables were microstructural (grain size, morphology, volume fraction and distribution of α and β phases). Any variation in results was therefore due to variations in microstructural resistance to fatigue crack initiation, brought about by the different heat treatments.

Post-sintering hydrogen-alloying treatments transformed the lamellar microstructure fully, by breaking up the continuous grain boundary α and colony structure. An extremely fine and homogeneous $\alpha + \beta$ microstructure was produced. Hydrogen-alloying treatments produced microstructures with smaller average α -grain sizes (0.91 to 1.26 μm) than equiaxed (3.4 μm) or lamellar microstructures (4.0 μm). As a result of refining the α -platelet thickness and reducing

the aspect ratio, significant ($p < 0.001$) increases in yield strength of up to 24% and increases in ultimate strength of up to 16% over the lamellar microstructure were attained. The yield and ultimate strengths were also 22% and 15% greater than the yield and ultimate strengths of the equiaxed microstructure recommended for surgical use [22].

The fatigue strengths of the hydrogen-alloyed microstructures were 29 to 35% greater than the fatigue strength of the lamellar microstructure. The reduced α -grain sizes of the hydrogen-alloy treated microstructures in comparison to the equiaxed microstructures resulted in a 9 to 13% increase in fatigue strength. The fatigue strengths attainable following hydrogen-alloy treatment therefore exceed the fatigue strengths of as-forged Ti-6Al-4V and are superior to fatigue strengths obtainable via other thermal cycling techniques [3, 7, 9, 13, 14].

Despite having small α -grains and aspect ratios, hydrogen-alloyed microstructures exhibited minimal necking, and did not exhibit the tensile ductility of the

TABLE III Mean tensile properties for different Ti-6Al-4V microstructures

Microstructure	YS (MPa)	UTS (MPa)	EL (%)	RA (%)
EA ($n = 6$)	914 (8)	1000 (14)	17.7 (0.2)	39.6 (1.0)
L ($n = 5$)	902 (53)	994 (33)	7.6 (1.4)	14.4 (3.5)
HAT-1 ($n = 4$)	1119 (53)	1152 (48)	2.8 (1.5)	11.3 (5.5)
HAT-2 ($n = 3$)	1011 (29)	1072 (21)	4.7 (1.3)	19.0 (3.2)
HAT-3 ($n = 6$)	974 (32)	1025 (48)	5.2 (0.9)	12.3 (2.8)

Standard deviations in ()

YS = yield strength, UTS = ultimate tensile strength, EL = elongation, RA = reduction in area

TABLE IV Results of Student's t-tests applied to tensile data

Microstructures	YS (MPa)	UTS (MPa)	EL (%)	RA (%)
EA-L	NS	NS	$p < 0.001$	$p < 0.001$
EA-HAT-1	$p < 0.001$	$p < 0.001$	$p < 0.001$	$p < 0.001$
EA-HAT-2	$p < 0.001$	$p < 0.001$	$p < 0.001$	$p < 0.001$
EA-HAT-3	$p < 0.005$	NS	$p < 0.001$	$p < 0.001$
L-HAT-1	$p < 0.001$	$p < 0.001$	$p < 0.001$	NS
L-HAT-2	$p < 0.025$	$p < 0.025$	$p < 0.05$	NS
L-HAT-3	$p < 0.05$	NS	$p < 0.025$	NS
HAT-1-HAT-2	$p < 0.05$	$p < 0.05$	NS	NS
HAT-1-HAT-3	$p < 0.005$	$p < 0.005$	$p < 0.05$	NS
HAT-2-HAT-3	NS	$p < 0.05$	NS	$p < 0.05$

NS = not significant at $p = 0.05$

TABLE V Mean fatigue strengths at $N = 10^7$ for different Ti-6Al-4V microstructures

Microstructure	σ_{fat} (MPa)	95% confidence interval (MPa)	$\sigma_{\text{fat}}/\sigma_{\text{UTS}}$
Equiaxed ($n = 15$)	590 (9)	{572 $\leq \mu \leq$ 609}	0.59
Lamellar ($n = 15$)	497 (7)	{484 $\leq \mu \leq$ 510}	0.50
HAT-1 ($n = 9$)	669 (51)	{570 $\leq \mu \leq$ 769}	0.58
HAT-3 ($n = 13$)	643 (7)	{629 $\leq \mu \leq$ 658}	0.63

Standard deviations in ()

TABLE VI Results of Student's t-tests applied to fatigue data

Microstructures	Level of significance
EA-L	$p < 0.001$
EA-HAT-1	NS
EA-HAT-3	$p < 0.005$
L-HAT-1	$p < 0.1$
L-HAT-3	$p < 0.001$
HAT-1-HAT-3	NS

NS = not significant at $p = 0.05$

morphologically similar equiaxed microstructure. This is because hydrogen-alloying treatments did not alter the prior β -grain size, only the refined α -grains within the prior β -grains formed into another morphology. Hydrogen-alloyed microstructures are still Widmanstätten microstructures. In other words, they are two-phase microstructures resulting from precipitation of α along preferred β crystallographic orientations. The slip characteristics of lamellar microstructures are therefore retained, and void formation and growth occurs along α - β interfaces and at Grain Boundary α . Another consequence of retaining the prior β -grain morphology was that the tensile properties were still subject to large scatter.

The question arises whether the superior strengths attainable through hydrogen-alloying treatments should be compromised to provide greater ductility. If required, a sub- β -transus ageing treatment following dehydrogenation can be performed. Also, higher dehydrogenation temperatures can be used and dehydrogenation times can be extended to coarsen the microstructure and increase ductility.

Annealing did not significantly reduce the yield and ultimate strengths. Annealing did, however, significantly ($p < 0.001$) reduce the total elongation and reduction in area by 57 and 64% respectively. Additionally, the mechanical properties of lamellar microstructures were subject to more scatter than the properties of the equiaxed microstructures. This is because lamellar microstructures were less homogeneous and had a more random grain orientation than equiaxed microstructures.

The relatively high fatigue strength of the equiaxed microstructure is attributed to the small α -grains and the randomly dispersed β -phase. These morphological characteristics minimize dislocation motion and slip. The combination of thicker, more elongated α -platelets, longer, more continuous regions of coherent α - β phase boundaries within platelet colonies, grain boundary α and heterogeneous prior β -grain orientation account for the lower fatigue strength of the lamellar microstructure in comparison to the equiaxed microstructure. The larger prior β -grain size in association with the crystallographic continuity across α - β boundaries increased the slip length, and slip was easily transmitted from one platelet to another across the α - β interfaces [2, 9].

The tensile and fatigue strengths reported here compare favourably with data from other hydrogen-alloying treatments performed on solid Ti-6Al-4V. Increases in tensile and fatigue strength of 15 to 20% have been reported for both mill annealed and cast Ti-6Al-4V treated with hydrogen [16].

Thermal cycles equivalent to the cycles of the hydrogen-alloying treatments, but without hydrogen, did not alter the lamellar microstructure. The increases in static and fatigue strength for the hydrogen-treated samples are therefore due to the phase transformations made possible by the temporary hydrogen-alloying, and not the thermal cycle itself.

Plotting yield, ultimate and fatigue strength as a function of α -grain size (Fig. 3), shows that Ti-6Al-4V follows a Hall-Petch relationship. Fitting the data of

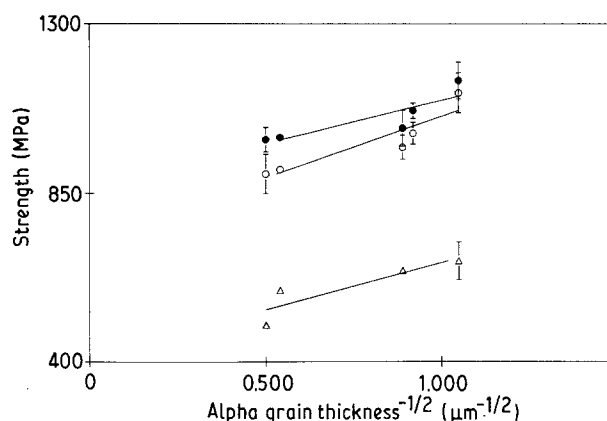


Figure 3 Plot of strength as a function of α -grain size for Ti-6Al-4V (● UTS, ○ YS, △ FAT·STR)

Tables II, III and V to an equation of the form

$$\sigma^* = \sigma_0 + kd^{-1/2} \quad (1)$$

where σ^* represents the yield strength, ultimate strength or fatigue strength, d the α -platelet thickness and σ_0 and k constants (Table VII) provides a quantitative means of determining the affect of α -grain size on static and fatigue strength.

Differences in the size and aspect ratio of the α -grains of the hydrogen-alloy treated microstructures were due to different amounts of growth during dehydrogenation. In addition to the refined α -platelet thicknesses, reduced platelet lengths also contributed to the increased fatigue strength, since the area of α - β interface continuity was reduced. A Hall-Petch criterion may therefore be used to explain structure-property relationships in titanium alloys, but the aspect ratios of the α -grains should also be considered.

The relationship between fatigue strength and microstructure is also determined through an analysis of fracture surface topography. The fracture characteristics of hydrogen-alloyed microstructures represent a combination of features seen in both equiaxed and lamellar microstructures. The fracture morphology as observed under SEM was planar, similar to the morphology of equiaxed microstructures. Fracture primarily occurred along α - β interfaces, a characteristic of lamellar microstructures. The analysis of the fractography of hydrogen-alloyed microstructures is facilitated by first summarizing the fracture characteristics of the equiaxed and lamellar microstructures.

Equiaxed samples contained a planar region of crack initiation. As crack length increased, the crack surface gradually changed to a more rounded, less planar surface with many microcracks perpendicular to the macroscopic crack front. Final fracture was

TABLE VII Hall-Petch parameters and correlation coefficients for Ti-6Al-4V strength data

σ^*	σ_0 (MPa)	k (MPa)	r
YS	728	328	0.92
UTS	869	231	0.87
σ_{fat}	311	317	0.78

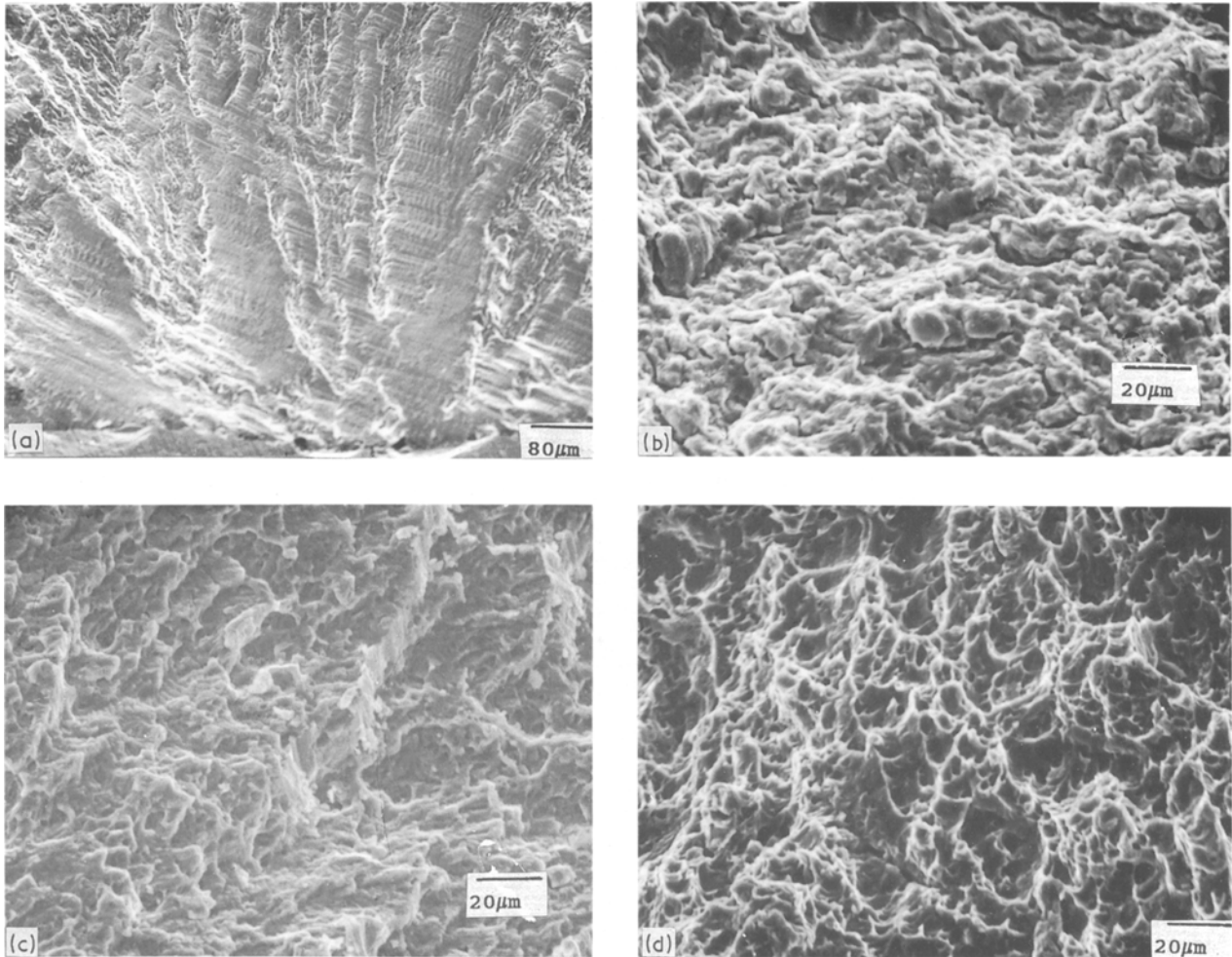


Figure 4 SEM photographs of HAT-3 treated Ti-6Al-4V fracture topography (a) crack initiation region $160 \times$ ($\sigma_{\max} = 655$ MPa, $N_f = 292\,400$), characterized by flat, faceted regions, having multiple crack fronts, (b) internal region, ($\sigma_{\max} = 638$ MPa, $N_f = 39\,700$), with rounded, ductile topology, and microcracks propagating perpendicular to the macroscopic front, (c) $a = 3$ mm ($\sigma_{\max} = 638$ MPa, $N_f = 39\,700$), small, locally striated regions were also present, (d) region of rapid fracture ($\sigma_{\max} = 655$ MPa, $N_f = 292\,400$), characterized by a dimpled morphology.

characterized by a dimpled morphology, signifying microvoid coalescence and ductile overload. Lamellar samples showed a flat, faceted fatigue crack initiation region. The predominant mode of early and mid-section failure in lamellar microstructures was cleavage, and as the crack advanced, regions of evenly spaced fatigue striations developed. Microcracks were prevalent in both cleaved and striated regions. Fatigue cracks through lamellar microstructures propagated parallel to the local α -colonies, along α - β interfaces and were more tortuous than cracks through equiaxed grains. Secondary microcracks propagated, and blunted, perpendicular to the local basketweave, providing steps which separated the different levels of primary crack propagation [27]. As the crack length increased, crack tortuosity increased, with the crack becoming highly jagged in the region of final fracture. These fracture surfaces of the equiaxed and lamellar microstructures confirm the fracture characteristics reported previously [1–3, 5, 6, 27, 28].

Fatigue crack initiation in hydrogen-alloyed microstructures was characterized by flat, faceted regions, having multiple crack fronts (Fig. 4a), typical of stage I fatigue fracture [29]. As the crack length and ΔK increased, there was a progressively changing topo-

graphy to a more rounded, ductile topology, with microcracks propagating perpendicular to the macroscopic front (Fig. 4b). Small, locally striated regions were also present (Fig. 4c). The fracture morphology then became completely dimpled (Fig. 4d), signifying rapid static fracture via ductile overload and rupture. The primarily uniform equiaxed shape of the dimples implies that a tensile stress was operative at the crack tip. These fracture features are reminiscent of the fracture surfaces of equiaxed titanium.

Fracture along the α - β interfaces in hydrogen-alloy treated microstructures presumably occurred because the strain intensification in the small α -grains was insufficient to produce failure prior to failure along α - β phase boundaries. This type of fracture contour is explained by the fact that hydrogen-alloy treated microstructures are very fine Widmanstätten microstructures with reduced aspect ratios, and Widmanstätten microstructures fail along α - β interfaces. There were local areas of transgranular fracture as well, and there were numerous undulations in the crack direction. As the crack length increased, the size and number of undulations increased, with the crack eventually becoming jagged. These fracture characteristics parallel some of the characteristics of lamellar titanium.

5. Summary and conclusions

The tensile and fatigue strengths attained through hydrogen-alloying are superior to the strengths attainable via other thermal cycling techniques and are amongst the highest strengths reported for Ti-6Al-4V. The superior fatigue strengths are a result of a far going refinement of microstructural lamellarity. Temporary alloying with hydrogen results in small α -grain sizes and reduced aspect ratios, and continuity of the α -phase at the prior β -grain boundaries is eliminated.

Three important conclusions were drawn from this research.

(1) The tensile and fatigue strengths of hydrogen-alloy treated Ti-6Al-4V are significantly greater than the strengths of β -annealed Ti-6Al-4V and also greater than the strengths of equiaxed Ti-6Al-4V. Therefore, β -annealing, β -sintering and casting may now be used without the associated reduction in fatigue strength.

(2) The tensile ductility of hydrogen-alloy treated Ti-6Al-4V is inferior to the ductility of equiaxed and lamellar microstructures. This is because the prior β -grain size was not refined and hydrogen-alloyed microstructures are still Widmanstätten microstructures. Some of the slip characteristics of lamellar microstructures are therefore retained and void formation and growth occurs along α - β interfaces and at grain boundary α .

(3) The fracture characteristics of the hydrogen-alloyed microstructures represent a combination of features seen in both equiaxed and lamellar microstructures. Fracture topography was similar to that of equiaxed samples, with flat, faceted regions changing to a more rounded, ductile topology, striated regions and a dimpled morphology, as crack length and ΔK increased. The fracture contour was similar to that of lamellar microstructures in that it primarily followed the α - β interfaces.

Acknowledgement

This research was made possible by a grant in aid from DePuy Inc, Warsaw, Indiana 46580, USA.

References

1. C. A. STUBBINGTON, *AGARD Conf. Proc. No. 185* (1976) p. 3.1.
2. H. MARGOLIN, J. C. WILLIAMS, J. C. CHESNUTT and G. LUTJERING, in *Titanium '80 Science and Technology*, Proceedings 4th International Conference on Titanium, Kyoto, May 1980, edited by H. Kimura and O. Izumi (The Metallurgical Society of AIME, Warrendale, PA, 1980) p. 169.
3. M. PETERS, A. GYSLER and G. LUTJERING, in *Titanium '80 Science and Technology*, Proceedings 4th International Conference on Titanium, Kyoto, May 1980, edited by H. Kimura and O. Izumi (The Metallurgical Society of AIME, Warrendale, PA, 1980) p. 1777.
4. G. LUTJERING and A. GYSLER, in *Titanium, Science and Technology*, Proceedings 5th International Conference on Titanium, Munich, September 1984, edited by G. Lutjering, U. Zwicker and W. Bunk (Deutsche Gesellschaft Fur Metallkunde, Oberursel, West Germany, 1985) p. 2065.
5. J. C. CHESNUTT, C. G. RHODES and J. C. WILLIAMS ASTM STP 600 (American Society for Testing and Materials, Philadelphia, 1976) p. 99.
6. R. E. LEWIS, J. G. BJELETICH, T. M. MORTON and F. A. CROSSLEY, ASTM STP 601 (American Society for Testing and Materials, Philadelphia, 1979) p. 371.
7. P. DUCHEYNE, D. KOHN and T. S. SMITH, *Biomat.* **8** (1987) 223.
8. J. J. LUCAS and P. P. KONIECZNY, *Met. Trans.* **2** (1971) 911.
9. C. A. STUBBINGTON and A. W. BOWEN, *J. Mater. Sci.* **9** (1974) 941.
10. S. M. SOLTESZ, R. J. SMICKLEY and L. E. DARDI, in *Titanium, Science and Technology*, Proceedings 5th International Conference on Titanium, Munich, September 1984, edited by G. Lutjering, U. Zwicker and W. Bunk (Deutsche Gesellschaft Fur Metallkunde, Oberursel, West Germany, 1985) p. 187.
11. J. GALANTE, W. ROSTOKER, R. LUECK and R. D. RAY, *J. Bone Joint Surg.* **53A** (1971) 101.
12. R. M. PILLIAR, *Clin. Orthop.* **176** (1983) 42.
13. D. EYLON, F. H. FROES and R. W. GARDINER, *J. Met.* **35** (1983) 35.
14. D. EYLON, F. H. FROES and L. LEVIN, in *Titanium, Science and Technology*, Proceedings 5th International Conference on Titanium, Munich, September 1984, edited by G. Lutjering, U. Zwicker and W. Bunk (Deutsche Gesellschaft fur Metallkunde, Oberursel, West Germany, 1985) p. 79.
15. W. R. KERR, P. R. SMITH, M. E. ROSENBLUM, F. J. GURNEY, Y. R. MAHAJAN and L. R. BIDWELL, in *Titanium '80 Science and Technology*, Proceedings 4th International Conference on Titanium, Kyoto, May 1980, edited by H. Kimura and O. Izumi (The Metallurgical Society of AIME, Warrendale, PA, 1980) p. 2477.
16. L. LEVIN, R. G. VOGT, D. EYLON and F. H. FROES, in *Titanium, Science and Technology*, Proceedings 5th International Conference on Titanium, Munich, September 1984, edited by G. Lutjering, U. Zwicker and W. Bunk (Deutsche Gesellschaft Fur Metallkunde, Oberursel, West Germany, 1985) p. 2107.
17. D. EYLON, C. F. YOLTON and F. H. FROES, in *Proceedings 6th World Conference on Titanium*, Cannes, June 1988, edited by P. Lacombe, R. Tricot and G. Beranger (Les Editions de Physique, Paris, 1989), p. 1523.
18. C. F. YOLTON, D. EYLON and F. H. FROES, in *Titanium Science Technology and Applications*, Proceedings 6th World Conference on Titanium, Cannes, June 1988, edited by P. Lacombe (Les Editions de Physique, Paris, 1989), in press.
19. D. H. KOHN and P. DUCHEYNE, in *Trans. 15th Annual Meeting of Society for Biomaterials*, Orlando, May 1989, p. 155.
20. D. H. KOHN and P. DUCHEYNE, *J. Mater. Sci.* (1990) (JMS MS 986-89).
21. W. H. KAO, D. EYLON, C. F. YOLTON and F. H. FROES, in "Progress in Powder Metallurgy", Vol. 37 (MPIF Publications, Princeton, 1981) p. 289.
22. ASTM standard F136-84, in "Annual Book of ASTM Standards, Vol 13.01: Medical Devices" (American Society for Testing and Materials, Philadelphia, 1987) p. 28.
23. ASTM standard E8-85b, in "Annual Book of ASTM Standards, Vol 3.01: Metals-Mechanical testing; Elevated and Low-Temperature Tests" (American Society for Testing and Materials, Philadelphia, 1987) p. 124.
24. ASTM standard E466-82, in "Annual Book of ASTM Standards, Vol 3.01: Metals-Mechanical testing; Elevated and Low-Temperature Tests" (American Society for Testing and Materials, Philadelphia, 1987) p. 571.
25. "ASTM Special Technical Publication 91-A" (American Society for Testing and Materials, Philadelphia, 1963).
26. J. A. COLLINS, "Failure of Materials in Mechanical Design" (John Wiley, New York, 1981).
27. "Metals Handbook", 9th Edn, Vol 12 (American Society of Metals, Metals Park, OH, 1979) p. 441.
28. P. E. IRVING and C. J. BEEVERS, *Mater. Sci. Engng* **14** (1974) 229.
29. G. F. V. VOORT, in "Metals Handbook", 9th Edn, Vol 12, (American Society of Metals, Metals Park, OH, 1979) p. 91.

Received 26 October
and accepted 8 November 1989